TO BE SUBMITTED
TO NUOVO CIMENTO

CERN/TC/PHYSICS 66-31
22nd December 1966

ANTIPROTON-PROTON ANNIHILATION INTO KAONS AND PIONS IN THE MOMENTUM REGION 3 to 4 GeV/c

B.R. French, J.B. Kinson, R. Rigopoulos* and V. Simak** - CERN, Geneva.

F. McDonald, G. Petmezas and L. Riddiford - University of Birmingham.

Abstract

A total of 1121 unambiguously identified events of the type $\bar{p}p \to \bar{K}Kn\pi$ (n = 1 - 5) at momenta 3.0, 3.6 and 4.0 GeV/c have been analysed, and partial cross-section for the various channels are given. The total cross-section for annihilation into two kaons with pions is estimated to be (5.1 ± 0.4) mb or 14% of all annihilations. The amount of resonant $K^*(890)$, ρ, ω, and associated K^*K^* production in the various channels are determined. Evidence for the E-meson, a $KK\pi$ resonance at 1700 MeV, and a $K^*\pi$ resonance at 1265 MeV is presented. Study of 955 unfitted events containing two charged particles, a K_1^0 and ≥ 2 neutral secondaries gives rise to a four standard deviation peak in a strangeness zero mass spectrum at (1820 ± 12) MeV with a width (Γ) of (50 ± 23) MeV.

The angular distributions favour a peripheral rather than a statistical or core-core model of the annihilation process. The possible usefulness of weighting the various combinations in accord with this observation, to accentuate enhancements in the invariant mass distribution, is discussed.

A method of separating each annihilation into its most likely two body final state configuration based on maximising the four momentum transfer (u) in the cross channel is presented as well as some examples of the enhancements in mass spectra obtained using this method.

---

* Visitor from Research Centre, Demokritos, Athens, Greece.

** Now at the Physics Institute of the Academy of Sciences, Prague, Czeckoslovakia.

1. Introduction

Preliminary results on the annihilation of 3.0 GeV/c momentum antiprotons into K's and π's have been reported previously[1], mainly for 5 and 6 body final states. In addition to the production of resonances, evidence has been observed for charge and hypercharge asymmetry in the angular distributions. Similar results have been reported by Baltay et al.[2,3] at 3.3 and 3.7 GeV/c. We have now extended our analysis to 3.6 and 4.0 GeV/c incident antiproton momenta, doubled the number of 2 prong interactions with a V^0 measured at 3,0 GeV/c, and studied the unfitted events with 2 prongs and one V^0. We shall discuss annihilations into $K\bar{K}$ and n pions, where n is 1 to 5.

The Saclay 81 cm hydrogen bubble chamber was exposed to a separated beam of antiprotons produced from an internal target in the CERN proton synchrotron. The momentum spread of the antiproton beam was $\pm$ 0.5 %, and a total of 300,000 photographs were taken containing 0.8×10^6, 0.5×10^6 and 1.1×10^6 antiprotons of momenta 3, 3.6 and 4 GeV/c respectively. From δ-ray counting and total cross-section measurements the contamination of the beam has been estimated to consist of 2 % pions and between 8 % and 12 % muons, depending on the incident antiproton momentum.

The film was scanned for events in which one or two K_1^0 decays ($K_1^0 \rightarrow \pi^+\pi^-$) were associated with an interaction having zero, two or four charged particles. From two independent scans, the overall scanning efficiency for these types of events was estimated to be 97 %. About 1,600 events at 3 GeV/c, 600 events at 3.6 GeV/c and 400 events at 4 GeV/c were measured by semiautomatic measuring machines, and their geometry and kinematics computed using the CERN programmes THRESH and GRIND. For the final analysis of the results, the programmes SLICE and SUMX were used.

2. Cross-sections and numbers of events

About 40 % of the events have more than one missing neutral particle (mainly the events with zero or two charged secondary particles). Of the remaining events 10 % were unmeasurable in the sense that a satisfactory geometrical reconstruction was not obtained after several remeasurements. Events were classified into the reactions shown in Tables I and II on the basis of the χ^2 calculated by the kinematics fitting programme. Where several interpretations were possible, ionisation estimates were made, thereby reducing the number of ambiguous events to less than 20 %. In the case of events where a single K_1^o was seen, about 50 % depended on ionisation estimates for unique identification. However the similarity in the numbers of events containing a K^+ or a K^- and in the reflected C.M.S. angular distributions of the K^+ and the K^- are an indication that no significant biases were introduced.

For each seen decay, a weight* was calculated to allow for the K_1^o's which decay either outside the fiducial volume of the chamber or less than 2 mm from the point of interaction. The average weights found were 1.22 and 1.14 for decays associated with two and four prong interactions respectively. The partial cross-sections at 3 GeV/c, which are listed in Table I, have also been corrected for unseen K^o decays (K_2^o decays and neutral K_1^o decays), scanning efficiency and the contamination of the beam; the density of the liquid hydrogen was taken to be 0.0625 gm/cm^3. Ambiguous and unmeasurable events have been taken into account in proportion to the unambiguous events.

In the calculation of cross-sections for the reactions involving $K^o\bar{K}^o$ pairs, events in which a single K_1^o decay was seen and the other inferred from the fit were used as well as those events where both K_1^o decays were seen. A correction was made for $K_2^o\bar{K}_2^o$ pairs assuming equal

---

* The weight is the true number of decays inferred from the observation of one decay.

production of K_1^o and $K_2^{o(\pm)}$; the unseen K^o's have been estimated to be composed of 25% K_1^o and 75% K_2^o. The cross-sections quoted for $K\bar{K}n\pi$ ($n = 1,2,3,4,5 \geq 6$) in the last column of Table III were calculated assuming equal production of $K^o\bar{K}^o$ and K^+K^- pairs for a given number of pions. The numbers of zero and two charged particle events with more than one π^o missing have been estimated by assuming that unfittable multineutral reactions of a given multiplicity have the same cross-sections as fittable reactions of higher prong number but with the same multiplicity. The cross-sections were also calculated from the observed numbers of fitted events using Clebsch-Gordan coefficients[4] and the results are the same within the statistical errors. We have observed no two body $K^o\bar{K}^o$ annihilations; the cross-section corresponding to one observed event would have been about 8 μb.

The total cross-section for all $K\bar{K}n\pi$ final states at 3 GeV/c has thus been estimated to be (5.1 ± 0.4) mb, which corresponds to 14% of the total annihilation cross-section.

3. Invariant mass distributions

Only events with 4, 5 or 6 particles in the final state have sufficiently good statistics for a detailed study of resonance production to be worthwhile. For events with a charged K, the third component of the isotopic spin (I_z) is known unambiguously for all combinations of particles, so that these events have been studied in more detail than those with a $K^o\bar{K}^o$ pair. Table IV lists the percentage production of $K^{\pm}$, ρ and ω^o at 3 GeV/c determined by fitting to the experimental histogram, using a least squares method, a curve consisting of Lorentz invariant phase space and a Breit-Wigner distribution with the known mass and width of the resonance. These are the only well-established resonances clearly seen in the present work. There is no evidence for the φ-meson.

(±) The probabilities of seeing 2, 1 and zero K_1^o's from a $K^o\bar{K}^o$ event are $(D/2W_n)^2$, $D(2W_n - D) / 2W_n^2$ and $(1 - \frac{D}{2W_n})^2$ respectively, D being the branching ration for charged K_1^o decays, and W_n the weight for a decay from an event of multiplicity n.

3.1. Invariant mass distributions for (Kπ) combinations

The (Kπ) combinations with $I_z = \pm 3/2$ give invariant mass distributions which agree well with the predicted phase space. For $I_z = \pm 1/2$ (Kπ) combinations the percentage production of K^*_{890} at 3 GeV/c in the various channels is shown in Table IV. The total $(K\pi)_{I_z = \pm 1/2}$ invariant mass distribution from the 4, 5 and 6 body events at all energies is shown in Figure 1. Fitting a composite phase space plus a Breit-Wigner curve to this distribution yields values for the mass and width of the K^* of (894 ± 5) MeV and (60 ± 10) MeV respectively.

3.2. Invariant mass distributions for (ππ) combinations

The percentage of $\rho^{\pm}_{0}$ production in the various channels at 3 GeV/c is shown in Table IV. A fit to the total $(\pi\pi)^{\pm}_{0}$ mass spectrum for all energies shown in Figure 2 yields values for the mass and width of the ρ of (744 ± 9) MeV and (98 ± 30) MeV. No significant deviations from phase space were seen for doubly charged combinations.

3.3. Invariant mass distributions for (πππ) combinations

For 5 and 6 body reactions three pion combinations with charge 1 or 2 give reasonable agreement with phase space (modified to include ρ production in the amounts given in Table IV). Of the two reactions which could show ω^0 production, the reaction $K^0\bar{K}^0\pi^+\pi^-\pi^0$ shows none, whereas for the reaction $K^0K^-\pi^+\pi^+\pi^-\pi^0$ with better statistics a clear ω^0 peak is seen in the $\pi^+\pi^-\pi^0$ mass spectrum corresponding to (15 ± 5)% of ω^0 production per event at 3 GeV/c. The mass and width of the ω^0 are found from the events at all energies, plotted in Figure 3, to be (790 ± 10) MeV and (17 ± 9) MeV respectively. The shaded region of Figure 3 shows that a large fraction of those events not having a $(\pi\pi)^{\pm}_{0}$ combination whose mass lies in the ρ region, (700 - 800) MeV, contain a $\pi^+\pi^-\pi^0$ mass lying in the ω^0 region.

3.4. Associated production of resonances

From the amounts of K^{*}, ρ and ω^{o} production given in Table IV it appears that the average number of resonances per event is approximately one, especially for the 5 and 6 body events with a $K^{\pm}$. We have therefore looked for associated production of these resonances. In the 4 and 5 body events, we estimate (after correction for the K^{*}'s which lie outside the selected mass interval and for the background under the K^{*} peak) that about zero and 20 ± 5 % respectively of the events contain two K^{*}'s in addition to those which may be expected from chance association of singly produced K^{*}'s. On the other hand no evidence for associated $K^{*}\rho$ production was observed in the 5 body events and no significant evidence for associated production of any kind was seen for the 6 body events.

3.5. The (KKπ) mass distribution

In the case of the 5 body final state $K^{o}K^{\pm}\pi^{\mp}\pi^{+}\pi^{-}$ the zero charged $(K^{o}K^{\pm}\pi^{\mp})$ mass distribution of events at all energies (Figure 4) shows evidence for the production of the E meson[5]. Fitting the distribution with phase space and a Breit-Wigner curve yields a mass and a width of (1423 ± 10) MeV and (45 ± 20) MeV respectively. The shaded histogram shows the $K^{o}K^{\pm}\pi^{\mp}$ mass distribution for those combinations in which a Kπ combination has a mass in the K^{*}_{890} region; the E-meson peak is then enhanced relative to the background.

Although of little significance as a single observation (~two standard deviations), the peak which can be seen in the $K^{o}K^{\pm}\pi^{\mp}$ mass distribution in the region 1675 - 1725 MeV is worth noting for the following reasons :

a) a small peak (~ 2 S.D) is also observed in the $K^{o}K^{\pm}\pi^{\mp}$ mass distribution in a similar experiment at 3.7 GeV/c[2,3], in the same mass interval as in the present experiment;

b) a peak is observed in the same mass interval (1.675 - 1.725) GeV in the $\rho^{o}\omega^{o}$ invariant mass spectrum from the reactions $\bar{p}p \rightarrow 3\pi^{+}3\pi^{-}\pi^{o}$ at 3 GeV/c, where appreciable ρ^{o} and ω^{o} production occurs[6];

c) a resonant state of mass (1700 $\pm$ 15) MeV and a narrow width with I spin $\geq$ 1 has been reported by Lovrat et al.[7].

The similarity of the mass, width and I-spin of the peaks in the $K^{*}K$ and $\rho^{o}\omega^{o}$ mass distributions suggests that they may represent different decay modes of this same object.

No evidence for the E-meson or the bump at 1700 MeV appears in the 5 body state $K^{o}\bar{K}^{o}\pi^{+}\pi^{-}\pi^{o}$, either for Q = 0 or Q = 1. However, as already stated, the value of I_z is uncertain for all (Kπ) combinations in this case.

3.6. The (K$\pi\pi$) mass distribution

Evidence has already been presented[8] for the possible existence in our data of a resonant (K$\pi\pi$) state with $I_z = \pm 3/2$ and mass 1270 MeV. This enhancement is observed only in the six body final state $K^{o}K^{\pm}\pi^{\mp}\pi^{+}\pi^{-}\pi^{o}$, and only in the pure I = 3/2 (K$\pi\pi$) combinations with $I_z = \pm 3/2$ (4 combinations/event) which contain a Kπ ($I_z = \pm 1/2$) combination in the $K^{*}(888)$ mass range. The fact that it has not been seen in the (K$\pi\pi$) combinations with $I_z = \pm 1/2$ could be due to the larger background (8 combinations/event) as well as to the fact that these combinations do not have pure isotopic spin. Figure 5a shows the $K^{*}\pi$ mass distribution with $I_z = \pm 3/2$ for all incident energies, the peak being slightly more statistically significant than reported previously at 3 GeV/c. The curve shown in Figure 5a is the best fit obtained using a $K^{*}\pi$ phase space and a Breit-Wigner which gives a mass and width of (1265 $\pm$ 10) MeV and (50 $\pm$ 20) MeV for the enhancement.

Of the 267 six-body events 60% (or 160 events) contain a K^{*}. Therefore of the 422 combinations in Figure 5a, 262 combinations are due to background. The 44 combinations in the 1265 MeV peak represent 27% of the 160 events containing a K^{*}.

Since there is evidence for considerable production of known resonances (K^{*}, ρ, ω^{o}) as well as peripheral effects (para. 4) in these

six body events, we attempted to study their influence on the $(K^{\pm}\pi)$ mass distribution. Five tracks were selected from different events, keeping the identity (including the charge) of the individual particles, and then one track at random was recalculated to conserve momentum only. Of the random events, those that conserved energy to within 100 MeV in the C.M.S. were analysed in the same way as the real events. By this procedure we were able to conserve the peripheral effects but largely destroy mass correlations between particles. The mass distributions from these events agree well with the calculated phase spaces, showing that any peripheral effects (see section four) do not appreciably influence the invariant mass distributions. In addition we have taken pions from one event and kaons from other events, so that the effects of the ρ and ω^{o} mesons produced in these interactions are retained but resonances involving kaons should be eliminated. The $(K^{\pm}\pi)$ mass distribution obtained by this procedure at 3 GeV/c is compared to that from the real events in Figure 5b, and demonstrates that the observed peak does not result from reflections due to the presence of ρ and ω mesons in these events.

3.7. Two prong events with more than one neutral particle

In addition to the fitted events, 955 unfitted events with two charged secondaries and a K_1^o have been studied. Each event was looked at on the scan table in an attempt to assign it to one of the following reactions, using the ionisation of the charged secondaries,

$$\bar{p}p \rightarrow K_1^o \pi^+ \pi^- [K^o] \; n \pi^o \qquad (1)$$

$$\rightarrow K_1^o K^+ \pi^- \; n \pi^o \qquad (2)$$

$$\rightarrow K_1^o \pi^+ K^- \; n \pi^o \qquad (3)$$

where $[K^o]$ represents an unseen K^o.

It was found that 183 events could be assigned uniquely to reaction (1), 475 events were ambiguous between either reactions (1) and (2) or (1) and (3) and 297 events were ambiguous between reactions (1), (2) and (3). Mass distributions were studied for the various possible combinations of particles. In addition to $K^{\pm}$ and ρ production a peak was

observed in the mass distribution of the K_1^o [K_o] n π^o combinations coming from the 955 events consistent with reaction (1). This distribution is shown in figure 6 and a peak of ~4 standard deviations significance is seen at a mass of (1820 $\pm$ 12) MeV, with a width (Γ) at half height of (50 $\pm$ 20) MeV. If this peak is due to a resonant state (J^o say) then it has strangeness zero and is produced in the reaction

$$\bar{p}p \rightarrow \pi^+ \pi^- J^o \quad \hookrightarrow K_1^o\,[K^o]\ n\ \pi^o \qquad (4)$$

Peaks in the $\rho^o\ \pi^+\ \pi^-$ and $\rho^o\ \omega^o$ mass distributions from the reactions

$$\bar{p}p \rightarrow \pi^+ \pi^- (\rho^o \pi^+ \pi^-)^o \qquad (5)$$

and

$$\bar{p}p \rightarrow \pi^+ \pi^- (\rho^o \omega^o)^o \qquad (6)$$

at (1834 $\pm$ 10) MeV and (1848 $\pm$ 11) MeV have been reported[6]. It is possible that one or both of these objects has the alternate decay mode, K_1^o [K^o] n π^o which gives rise to the peak observed here(*).

4. Angular distributions

In the $K^o\bar{K}^o n\pi$ events the K^o and $\bar{K}^o$ cannot be distinguished, and consequently the angular distribution in the C.M.S. of the $K^o(\bar{K}^o)$ should be symmetric about 90°, as is found experimentally. The $K^{\pm}K^o n\pi$ final states are more interesting since the K^o can be identified as a particle or antiparticle according to the charge of the other kaon. The $\pi^{\pm}$, π^o distributions for the 4, 5 and 6 body states with no charged kaons agree, within the poorer statistical errors, with those for the charged kaon events (Figure 7).

As pointed out in section 2, the correct identification of the events depends to a considerable extent on ionisation measurements, which could produce biases in the angular distributions in the C.M.S. However

(*) In principle by studying the mass spectrum of $K_1^o\ K_1^o$ n π^o in the events $K_1^o K_1^o \pi^+ \pi^-$ n π^o we should be able to give some information about the C-parity. However these events have not been analysed.

we know from the C-symmetry of the $\bar{p}p$ interaction[9] that the angular distribution of a particle with respect to the proton should be identical to that of the antiparticle with respect to the antiproton. For the three, five and six body final states the angular distributions of the K^+ and the K^- reflected about 90° in the C.M.S. agree well; also the numbers of events found to have a K^+ or a K^- are equal within the statistical errors. In the case of the four body final state $K^\pm K^\circ \pi^\mp \pi^\circ$ however, the K^+ angular distribution is more peaked in the backward direction in the C.M.S. than the reflected K^- distribution. In addition fewer events are observed with a K^- than a K^+, although the difference is not very significant. Both of these observations are consistent with the bias which might be expected in the one constraint fit class because of the difficulty in identifying high energy charged kaons from pions, if the $K^-(K^+)$ are produced preferentially forwards (backwards) in the C.M.S. (see Table V). As a result, the addition of the K^+ and the reflected K^- angular distributions in the C.M.S. probably underestimates the asymmetry of the C.M.S. angular distribution for the four body events with a charged kaon. In the three body events $K^+K^\circ\pi^-$, which are four constraint fits, no biases are seen.

The C.M.S. angular distributions of particles with the reflected angular distributions of the antiparticles added are shown in Figures 7a and 7b for 3, 4, 5 and 6 body final states containing a charged kaon; ρ-meson distribution would not be accurate because of the large background (Figure 2). Evidence for asymmetry of these angular distributions can be seen. The ratio of the number of particles emitted forward in the C.M.S. ($\cos\theta^* > 0$) to the number emitted backwards is summarised for the different reactions, particles and charges in Table V. The dependence of the angular distribution of pions, kaons and K^*'s on the incident antiproton momentum can be seen in Figure 8 where the distributions at 3 GeV/c have been compared with those at 3.6 and 4 GeV/c taken together. The angular distributions for the K^* were obtained from the angular distribution of the $(K\pi)$ mass conbinations in the mass interval 830 - 945 MeV after subtracting the angular distribution of $(K\pi)$ combinations in adjacent mass intervals corresponding to the background distribution. The angular distribution of the ω° meson was obtained in a similar way using a mass interval for the ω° of 740 - 820 MeV.

From Table V, figures 7 and 8(*), and the associated work, one may draw the following conclusions :

a) the asymmetry in the C.M.S. angular distributions decreases as the number of bodies in the final state increases;

b) the asymmetry increases with the momentum of the incident antiproton;

c) charged particles show more asymmetry than neutral ones;

d) the angular asymmetry (where pertinent) and collimation are more pronounced for the heavy particles (K^{*}, K, ω^{o}) than for the light ones (π), and the resonances K^{*}, ω^{o} are more collimated (that is appear more preferentially in the polar than the equatorial hemispheres), than the Kπ or $\pi^{+}\pi^{-}\pi^{o}$ combinations in adjacent mass regions.

These observations are incompatible with a simple statistical model of the annihilation process, which would predict a symmetric angular distribution in the C.M.S. In the Koba-Takeda model[10] of antiproton-proton annihilation and its extension by Stajano[11,12] the heavier particles are expected to be produced mainly in the core-core annihilations which would involve the lower angular momentum states, and therefore the angular distributions of the heavier particles should be more isotropic and symmetric than for the lighter particles. The observations are otherwise and seem to favour an annihilation mechanism involving peripheral interactions. Such a model requires the exchange of a fermion (hyperon in our case) and the only relevant theoretical work, to our knowledge, is that of Pilkuhn[13] who showed that the data at 1.61 GeV/c[14] was more consistent with a peripheral model than with the Koba-Takeda model.

(*) Corrections for weights are not made in figures 7 and 8 and Table V. However the variations in weights about their mean values, together with the checks on the equality between numbers of events and their charge conjugates and of the particle and reflected antiparticle C.M.S. angular distributions, suggest that the results and conclusions of this section (and the preceding one) are unlikely to be seriously affected.

5.1. Peripheral production of resonances

As has been pointed out in section 4, the angular distributions of resonance states are peaked towards $\cos \theta^{*} = \pm 1$ in the C.M.S.; also the forward/backward ratios (Table V) are larger the greater the mass of the state. In an attempt to exploit these facts we have tried various procedures to enhance the likelihood of detecting peaks in invariant mass spectra. Thus we have tried weighting each mass combination by a factor W where :-

a) $W = p^{*} / p^{*}_{max}$ where p^{*} is the actual momentum of the particle combination in the C.M.S., and p^{*}_{max} is the maximum value of momentum found amongst all possible particle combinations ;

b) $W = u/u_{max}$, where u is the four momentum transfer to the incident proton in the case of an antiparticle combination and to the antiproton for a particle combination. In the case of annihilation interactions we have found u to be more sensitive than t, the usual four momentum transfer ; and

c) $W = \cos \theta^{*}$ or $\cos^{6} \theta^{*}$, where θ^{*} is the emission angle of the particle combination in the C.M.S., and the power six was arbitrarily chosen to enhance any possible effect.

From a mass point of view weighting with a function of $\cos \theta$ is less biased than using a function of p^{*} or u and Figure 9 shows the $\bar{K}^{o} K^{+}$ + c.c. mass distribution for all energies from the 4, 5 and 6 body reactions, both unweighted and weighted as $\cos^{6} \theta^{*}$ ($\cos^{6} \theta$ was chosen since the $K^{*}(888)$ angular distribution follows roughly this form). The weighted distribution beings out from background two small peaks at 1.05 and 1.25 GeV, already observed in a stopping antiproton experiment[15], plus another as yet unobserved peak at 1740 MeV, unless it could correspond to that observed at 1748 MeV by Levrat et al.[7].

5.2. The method of maximum $|t|$

As a further attempt to exploit the apparently peripheral nature of the events, we have used a criterion to divide each event into a unique configuration consisting of two bodies. The criterion was such that the configuration chosen was that in which a combination of particles had the maximum $|t|^{(\pm)}$ value; the remaining combination of particles having, of course, the same $|t|$ value. Some examples of the results are shown in figures 10 - 14, more for their interesting features than for their statistical significances. Maximum $|t|$ was used rather than minimum $|t|$ since it was found that more structure appeared in mass spectra using the latter than the former.

Figure 10 shows the results for the reaction $\bar{p}_l \rightarrow K^+ \bar{K}^o_1 \pi^- + c.c.$ The events in which the $(K^o_1 \pi^\pm)$ combination has the maximum value of $|t|$ have a $(K^o_1 \pi^\pm)$ mass spectrum concentrated in the mass region of the $K^\pm(888)$, whereas the events in which the $(K^\pm \pi^\mp)$ combination has the maximum $|t|$ value have $(K^\pm \pi^\mp)$ masses which are grouped at a higher mass centred at 1.32 GeV$^{(+)}$. There is no obvious reason, à priori, why the neutrally charged combinations should prefer higher mass values than the charged combinations. However, if one assumes that annihilation proceeds via the exchange of Λ^o or $\Sigma^{\pm o}$ hyperons then SU_3 Clebsch-Gordon coefficients predict a ratio of $K^{*\pm}(888) / K^{*o}(888) = 4$, whereas the observed ratio below 1000 MeV is ~ 6.

Figure 11a shows the mass distribution of the $(K\pi\pi)$ combinations which have maximum $|t|$ in the reaction $\bar{p}p \rightarrow K^+ K^o_1 \pi^- \pi^o + c.c.$ A concentration of events in a relatively small mass range with a central value of

---

(±) $t = (\vec{P}_i - \vec{P}_f)^2 - (E_i - E_f)^2$, where $\vec{P}_i$ and E_i are the momentum and energy of the incident antiproton or proton and $\vec{P}_f$ and E_f are the momentum and energy of the particle or group or particles considered.

(+) Evidence for a $(K\pi\pi)$ resonance at 1.32 GeV has been reviewed by Goldhaber[16].

1.27 GeV is seen(*). The $(K^0_1 K^{\pm})$ mass distribution for the events in which the $(K^0_1 K^{\pm})$ combination has the maximum $|t|$ value is shown in Figure 11b and a peak is seen at a mass of 1.26 GeV similar to that observed by Armenteros et al.(15).

Figure 12a shows the $(K^{\pm} K^0_1 \pi^{\mp})$ mass distribution from the reaction $\bar{p}p \to K^{\pm} K^0_1 \pi^{\mp} \pi^+ \pi^-$ under the $|t|$ selection criterion almost all events lie in the region of the E-meson. In fact there are 17 events in the peak above the background whereas in the corresponding mass distribution without the selection criterion (figure 4) there were 19 events above background. Thus in this case the signal to noise ratio has been appreciably enhanced. The angular distribution of the $(K^{\pm} K^0_1 \pi^{\mp})$ combinations having a mass in the region of the E-meson is shown in figure 12b, and is seen to be quite anisotropic as is to be expected from the method of selection. The total $(K^{\pm} K^0_1 \pi^{\mp})$ mass spectrum, obtained in a similar way, for the 4, 5 and 6 body reactions is shown in figure 12c where the concentration of events in the E-meson region is more significant. If for the 6 body events the mass of the remaining $\pi^+\pi^-\pi^0$ combination is plotted against the $K^{\pm} K^0_1 \pi^{\mp}$ mass (figure 12d) a cluster of points is seen at a position corresponding to the reaction $\bar{p}p \to E^0 \omega^0$.

It is clear that with the above method of selection the mass distributions obtained show more structure than the total mass distributions and the following argument may give an explanation why this is so. The annihilation cross-section at 3 GeV/c is of the order of 30 mbs, a cross-section which implies a minimum radius of interaction (r) of one fermi (10^{-13} cms). Therefore since the incident proton (or antiproton) momentum in the C.M.S. (p^*) is 1 GeV/c, angular momenta up to at least five may be involved in the annihilation channels ($p^* r \simeq \ell h$). However the single particle angular distributions in the C.M.S. are not very anisotropic and

---

(*) It is possible that this peak is related to the peak in the $(K\pi\pi)$ $T_Z = \pm 3/2$ mass spectrum at 1.27 GeV observed in the reaction $\bar{p}p \to K^+ K^0_1 \pi^+ \pi^- \pi^- \pi^0$ + c.c. and discussed in section 3.6.

do not reflect the angular distributions expected from the primary products of an interaction involving such high values of ℓ. A simple explanation of this apparent anomaly is found if the primary products of the interaction are concentrated in two centres whose relative angular momentum is large (e.g. a peripheral exchange diagram involving nucleon or hyperon exchange) and which subsequently decay with a sufficiently high Q-value that the angular distribution of the decay products washes out the original angular distribution of the two centres. The two centres are then obvious sources for resonance production and could explain why the method of maximum u selection enhances the likelihood of seeing these resonances.

Acknowledgements

We would like to express our gratitude to our scanning and measuring staffs and to the personnel of the T.C. division who built and operated the beam. Thanks are also due to Dr. R.A. Armenteros for valuable criticisms and Prof. Ch. Peyrou for his constant encouragement and support.

o o

o

REFERENCES

1. B.R. French, J.B. Kinson, V. Simak, J. Badier, M. Bazin, A. Rougé and P. Grieve. Report to the International Conference on High Energy Physics, Dubna (1964).

2. C. Baltay, J. Lach, J. Sandweiss, H. Taft, N. Yeh, D.J. Crennell, Y. Oren, C.R. Richardson, D.L. Stonehill and R. Stump. Report to the International Conference on High Energy Physics, Dubna (1964).

3. C. Baltay, J. Lach, J. Sandweiss, H.D. Taft, N. Yeh, D.L. Stonehill, and R. Stump. Phys.Rev. 142, 932 (1966).

4. J. Vandermeulen, CERN Report DD/IEP/61/29, 1961, which uses results from F. Cerulus, Nuovo Cimento 19, 528 (1961) and Suppl. Nuovo Cimento 15, 402 (1960) ; and from Y. Yeivin and A. de Shalit, Nuovo Cimento 1, 1147 (1955).

5. R. Armenteros, D.N. Edwards, T. Jacobsen, A. Shapira, J. Vandermeulen, Ch. d'Andlau, A. Astier, P. Baillon, H. Briand, J. Cohen-Ganouna, C. Defoix, J. Siaud, C. Ghesquiere and P. Rivet. Proceedings of the Sienna International Conference on Elementary Particles 1, 287 (1963).

6. J.A. Danysz, B.R. French, and V. Simak. CERN/TC/PHYSICS 67-1.

7. B. Levrat, C.A. Tolstrup, B. Schubelin, C. Nef, M. Martin, B.C. Maglić, W. Kienzle, M.N. Focacci, L. Dubal and G. Chikovani, Phys. Lett. 22, 714 (1966).

8. R. Böck, B.R. French, J.B. Kinson, V. Simak, J. Badier, M. Bazin, B. Equer and A. Rougé. Phys. Lett. 12, 65 (1964).

9. A. Pais, Phys.Rev.Letters 3, 242 (1959).

10. Z. Koba and G. Takeda. Prog.Theor.Phys. 19, 269 (1958).

11. A. Stajano, Nuovo Cimento, 24, 774 (1962).

12. A. Stajano, Nuovo Cimento, 28, 197 (1963).

13. H. Pilkuhn, Arkiv für Fysik, 23, 259 (1962).

14. G.R. Lynch, Rev.Mod.Phys. 33, 395 (1961).

PS/5750/dmh

REFERENCES (contd.)

15. R. Armenteros, D.N. Edwards, T. Jacobsen, L. Montanet, J. Vandermeulen, Ch. d'Andlau, A. Astier, P. Baillon, J. Cohen-Ganouna, C. Defoix, J. Siaud and P. Rivet. Phys. Lett. 17, 344 (1965).

16. M. Goldhaber, Rapporteur's talk at the Berkeley Conference, Sept. (1966).

TABLE I

Partial cross sections for $\bar{p}p \rightarrow \bar{K}K + n\pi$ at 3 GeV/c					
n	Reaction Observed	No. of Events (***)	μb/ /event (****)	σ(μb) calculated for reaction	
1	$K_1^0 K_1^0 \pi^0$	2.4	0.6	20 ± 15	$K^0\bar{K}^0\pi^0$
1	$K_1^0 K^\pm \pi^\mp$	12	1.5	65 ± 20	$K^0 K^\pm \pi^\mp$
2	$K_1^0 K^\pm \pi^\mp \pi^0$	99.5	1.5	550 ± 60	$K^0 K^\pm \pi^\mp \pi^0$
2(**)	$K_1^0 (K^0) \pi^+ \pi^-$ (*)	41.5	1.5	158 ± 30	$K^0\bar{K}^0\pi^+\pi^-$
2	$K_1^0 K_1^0 \pi^+ \pi^-$ (*)	35	0.6	280 ± 45	$K^0\bar{K}^0\pi^+\pi^-$
3	$K_1^0 K_1^0 \pi^+ \pi^- \pi^0$	69	0.6	555 ± 70	$K^0\bar{K}^0\pi^+\pi^-\pi^0$
3	$K_1^0 K^\pm \pi^\mp \pi^+ \pi^-$	176	0.6	355 ± 30	$K^0 K^\pm \pi^\mp \pi^+ \pi^-$
3	$K_1^0 K^\pm \pi^\mp \pi^+ \pi^- \pi^0$	234	0.6	475 ± 40	$K^0 K^\pm \pi^\mp \pi^+ \pi^- \pi^0$
4(**)	$K_1^0 (K^0) \pi^+ \pi^- \pi^+ \pi^-$ (≠)	72	0.6	105 ± 14	$K^0\bar{K}^0\pi^+\pi^-\pi^+\pi^-$
4	$K_1^0 K_1^0 \pi^+ \pi^- \pi^+ \pi^-$ (≠)	21.5	0.6	152 ± 34	$K^0\bar{K}^0\pi^+\pi^-\pi^+\pi^-$
5	$K_1^0 K_1^0 \pi^+ \pi^- \pi^+ \pi^- \pi^0$	15	0.6	100 ± 30	$K^0\bar{K}^0\pi^+\pi^-\pi^+\pi^-\pi^0$
6	$K_1^0 K_1^0 \pi^+ \pi^- \pi^+ \pi^- m\pi^0$, $m \geq 2$	4.5	0.6	30 ± 20	$K^0\bar{K}^0\pi^+\pi^-\pi^+\pi^- m\pi^0$, $m \geq 2$

The two reactions (*) should yield the same cross-sections, as should the two reactions (≠), if $K_1^0 K_1^0$ and $K_1^0 K_2^0$ are produced equally.

(**) (K^0) signifies a missing K^0 determined by the fit procedure.

(***) Includes ambiguous and unmeasurable events (see text).

(****) The numbers of events are not all from the same amount of film.

TABLE II

Numbers of unambiguous events used in the figures, and Tables III and IV

Reaction	Primary momentum (GeV/c) 3.0	3.6	4.0	Total No. of events	
$\bar{K}^o_1 K^+ \pi^-$	10	5	6	21	47
$K^o_1 K^- \pi^+$	15	9	2	26	
$\bar{K}^o_1 K^+ \pi^- \pi^o$	60	26	23	109	196
$K^o_1 K^- \pi^+ \pi^o$	58	9	20	87	
$K^o_1(\bar{K}^o) \pi^- \pi^+$ (*)	49	24	20		93
$K^o_1 \bar{K}^o_1 \pi^- \pi^+$	35	10	20		65
$\bar{K}^o_1 K^+ \pi^- \pi^- \pi^+$	67	25	7	99	200
$K^o_1 K^- \pi^+ \pi^+ \pi^-$	70	25	6	101	
$K^o_1 \bar{K}^o_1 \pi^+ \pi^- \pi^o$	63	32	51		146
$\bar{K}^o_1 K^+ \pi^- \pi^- \pi^+ \pi^o$	91	36	8	135	267
$K^o_1 K^- \pi^+ \pi^+ \pi^- \pi^o$	91	31	10	132	
$K^o_1(\bar{K}^o) \pi^- \pi^- \pi^+ \pi^+$ (*)	56	22	4		82
$K^o_1 K^o_1 \pi^- \pi^- \pi^+ \pi^+$	20	4	1		25
Total	685	258	178		1121

(*) (K^o) signifies a missing K^o determined by the fit procedure.

TABLE III

Partial Cross-sections for $\bar{p}p \rightarrow K\bar{K} + n\pi$ at 3 GeV/c

n	Reaction	Numbers of Event Types *			Cross section (mb) **
		Seen and Fittable	Seen and not Fittable	"Unseen"	
1	$K\bar{K}\pi$	2	0	1	0.11 ± 0.03
2	$K\bar{K}\pi\pi$	2	1	2	1.0 ± 0.1
3	$K\bar{K}\pi\pi\pi$	2	2	2	1.8 ± 0.2
4	$K\bar{K}\pi\pi\pi\pi$	2	3	3	1.4 ± 0.2
5	$K\bar{K}\pi\pi\pi\pi\pi$	2	4	3	0.6 ± 0.2
6	$K\bar{K}n\pi$	2	5	3	0.2 ± 0.2
7	$K\bar{K}n\pi$	2	6	3	
Total	7	14	21	17	5.1 ± 0.4

* Assumes no events with more than 6 charged prongs; also charge conjugates are not counted separately.

** It is assumed that there are no errors in the method of estimating the cross-sections for "unseen" events (those with K^+K^-) or those which cannot be fitted (that is, have more than one neutral pion).

TABLE IV

Production of K^{*}, ρ and ω at 3.0 GeV/c

Particles in the final state.	No. of ($K\pi$) combinations/ event	% K^{*} production per event	No. of ($\pi\pi$) combinations/ event with charge 0 or 1	% ρ production per event	% ω^{o} production per event
$K^{o}K^{o}\pi^{+}\pi^{-}$	4	30 ± 12	1	15 ± 10	-
$K^{o}K^{\pm}\pi^{\mp}\pi^{o}$	4	15 ± 10	1	10 ± 10	-
$K^{o}K^{o}\pi^{+}\pi^{-}\pi^{o}$	6	50 ± 20	3	40 ± 20	0
$K^{o}K^{\pm}\pi^{\mp}\pi^{+}\pi^{-}$	4 with $T_z = \pm 1/2$	60 ± 15 *	2	35 ± 10	-
$K^{o}K^{o}\pi^{+}\pi^{+}\pi^{-}\pi^{-}$	8	50 ± 30	4	30 ± 20	-
$K^{o}K^{\pm}\pi^{\mp}\pi^{+}\pi^{-}\pi^{o}$	6 with $T_z = \pm 1/2$	60 ± 10	5	50 ± 20	15 ± 5

* Because of associated production, this implies that $(40 \pm 12)\%$ of all events have one or two K^{*}'s.

TABLE V

FORWARD/BACKWARD RATIOS

Reaction	$\pi^- + (\pi^+)_R$	$K^-, \bar{K}^0 + (K^+, K^0)_R$	$K^{*-}, \bar{K}^{*0} + (K^+, K^{*0})_R$
$\bar{K}^0 K^+ \pi^-$ $K^0 K^- \pi^+$	1.9 ± 0.4	2.9 ± 0.4	-
$\bar{K}^0 K^+ \pi^- \pi^0$ $K^0 K^- \pi^+ \pi^0$	2.0 ± 0.3	2.2 ± 0.2	2.5 ± 0.6
$\bar{K}^0 K^+ \pi^- \pi^+ \pi^-$ $K^0 K^- \pi^+ \pi^+ \pi^-$	1.10 ± 0.07	1.8 ± 0.2	2.9 ± 0.5
$\bar{K}^0 K^+ \pi^- \pi^+ \pi^- \pi^0$ $K^0 K^- \pi^+ \pi^+ \pi^- \pi^0$	1.1 ± 0.1	1.2 ± 0.1	0.8 ± 0.3
all reactions at 3.0 GeV/c	1.19 ± 0.03	1.48 ± 0.07	1.61 ± 0.2
all reactions at 3.6 and 4.0 GeV/c	1.22 ± 0.08	1.86 ± 0.15	2.1 ± 0.3
K, K^* $(Q = 0)$	-	1.4 ± 0.1	1.33 ± 0.2
$\pi, K, K^*(Q = \pm 1)$	1.20 ± 0.015	1.8 ± 0.1	2.7 ± 0.4
Total	1.20 ± 0.05	1.60 ± 0.04	1.9 ± 0.2

Figure Captions

Fig. 1. ($K\pi$) mass distribution. The thick line histogram is from reactions $\bar{K}^0_1 K^+ n\pi$ and $K^0_1 K^- n\pi$ and with $|I_z| = 1/2$; the thin line histogram includes reactions $K^0\bar{K}^0 n\pi$. The dashed curve is phase space and the full line is phase space plus a Breit-Wigner distribution.

Fig. 2. ($\pi\pi$) with $I_z = 0, \pm 1$ mass distribution from all reactions. The thick line histogram is the mass distribution of $(\pi^+\pi^-)$ and the thin line includes that of $(\pi^\pm\pi^0)$. The dashed curve is phase space and the full line is phase space plus a Breit-Wigner distribution.

Fig. 3. $(\pi^+\pi^-\pi^0)$ mass distribution for reactions $\bar{K}^0_1 K^+ \pi^- \pi^+ \pi^- \pi^0$ and $K^0_1 K^- \pi^+ \pi^+ \pi^- \pi^0$. The thick line histogram corresponds to reactions where there is no $(\pi^+\pi^-)$ or $(\pi^\pm\pi^0)$ mass combination in the ρ interval (700 - 800 MeV). The dashed curve is phase space and the full line is phase space plus a Breit-Wigner distribution.

Fig. 4. $\bar{K}^0_1 K^+ \pi^-$ and $K^0_1 K^- \pi^+$ mass distribution from the reactions $\bar{K}^0_1 K^+ \pi^- \pi^+ \pi^-$ and $K^0_1 K^- \pi^+ \pi^+ \pi^-$. The thick line histogram is the mass distribution of $(K^{*\pm} K^\mp)$ which has $I_z = 0$. The dashed curve is phase space and the full line is phase space plus a Breit-Wigner distribution.

Fig. 5. a) $(K^{*\pm}\pi^\mp)$ with $I_z = \pm 3/2$ mass distribution for reactions $\bar{K}^0_1 K^+ \pi^- \pi^+ \pi^- \pi^0$ and $K^0_1 K^- \pi^+ \pi^+ \pi^- \pi^0$. The thick line histogram corresponds to the $K^{*\pm}\pi^\mp$ combinations. The dashed curve is phase space and the full line is phase space plus a Breit-Wigner distribution.

b) $(K^{*\pm}\pi^\mp)$ with $I_z = \pm 3/2$ mass distribution for the same reaction as in Fig. 5a but with 3.0 GeV/c primary momentum of antiprotons only. The thin line histogram represents Monte-Carlo events with ρ and ω included (see text), and the thin line curve is phase space.

Fig. 6. Mass distribution of K^0_1 [K_0] $n\pi^0$ combinations from events consistent with the interpretation $\bar{p}p \rightarrow \pi^+\pi^- K^0_1[K^0] n\pi^0$.

Figure Captions (contd.)

Fig. 7. a) Angular distributions of $\bar{K}^0$ plus reflected K^0, K^- plus reflected K^+, and π^- plus reflected π^+, for 3, 4, 5 and 6 body final states respectively, each containing a charged kaon.

b) Angular distributions of π^-, $\bar{K}^0$, K^-, $\bar{K}^{*0}$, K^{*-} (including reflected distributions of π^+, K^0, K^+, K^{*0}, K^{*+}) for the sums of 3, 4, 5 and 6 body final states containing a charged kaon. Angular distributions for π^0's and ω^0's are symmetrized around $\cos\theta^* = 0$.

Fig. 8. Angular distributions of π's, K's and K^*'s for primary momenta of antiprotons 3.0 and 3.6 plus 4.0 GeV/c respectively.

Fig. 9. a) Histogram of $\bar{K}^0_1K^+$ and $K^0_1K^-$ effective masses with normalized phase space curve.

b) Weighted histogram of $\bar{K}^0_1K^+$ and $K^0_1K^-$ with $W = \cos^6\theta^*$ normalized to the same area as on Fig. 9a.

Fig. 10. Constant area ideogram of the $(K^\pm\pi^\mp)$ and $(K^0_1\pi^\pm)$ effective masses having maximum u in the reaction $\bar{p}p \rightarrow K^0_1K^\pm\pi^\mp + c.c.$

Fig. 11. Constant area ideogram of the $(K\pi\pi)$ and $(K^0_1K^\pm)$ effective masses having maximum u in the reaction $\bar{p}p \rightarrow \bar{K}^0_1K^\pm\pi^\mp\pi^0 + c.c.$

Fig. 12. a) Constant area ideogram of the $(K^0_1K^\pm\pi^\mp)$ effective masses having maximum u in the reaction $\bar{p}p \rightarrow \bar{K}^0_1K^+\pi^+\pi^-\pi^- + c.c.$

b) C.M.S. angular distribution of the $(K^0_1K^\pm\pi^\mp)$ combination having maximum u in the reaction $\bar{p}p \rightarrow K^0_1K^+\pi^+\pi^-\pi^- + c.c.$

c) Constant area ideogram of the $(K^0_1K^\pm\pi^\mp)$ effective masses having maximum u in the reactions $\bar{p}p \rightarrow \bar{K}^0_1K^+\pi^-\pi^0 + c.c.$

$\rightarrow \bar{K}^0_1K^+\pi^+\pi^-\pi^- + c.c.$

$\rightarrow \bar{K}^0_1K^+\pi^+\pi^-\pi^-\pi^0 + c.c.$

d) Scatter plot of the $(K^0_1K^\pm\pi^\mp)$ mass versus $(\pi^+\pi^-\pi^0)$ mass under maximum u selection for the reaction $\bar{p}p \rightarrow \bar{K}^0_1K^+\pi^+\pi^-\pi^-\pi^0 + c.c.$

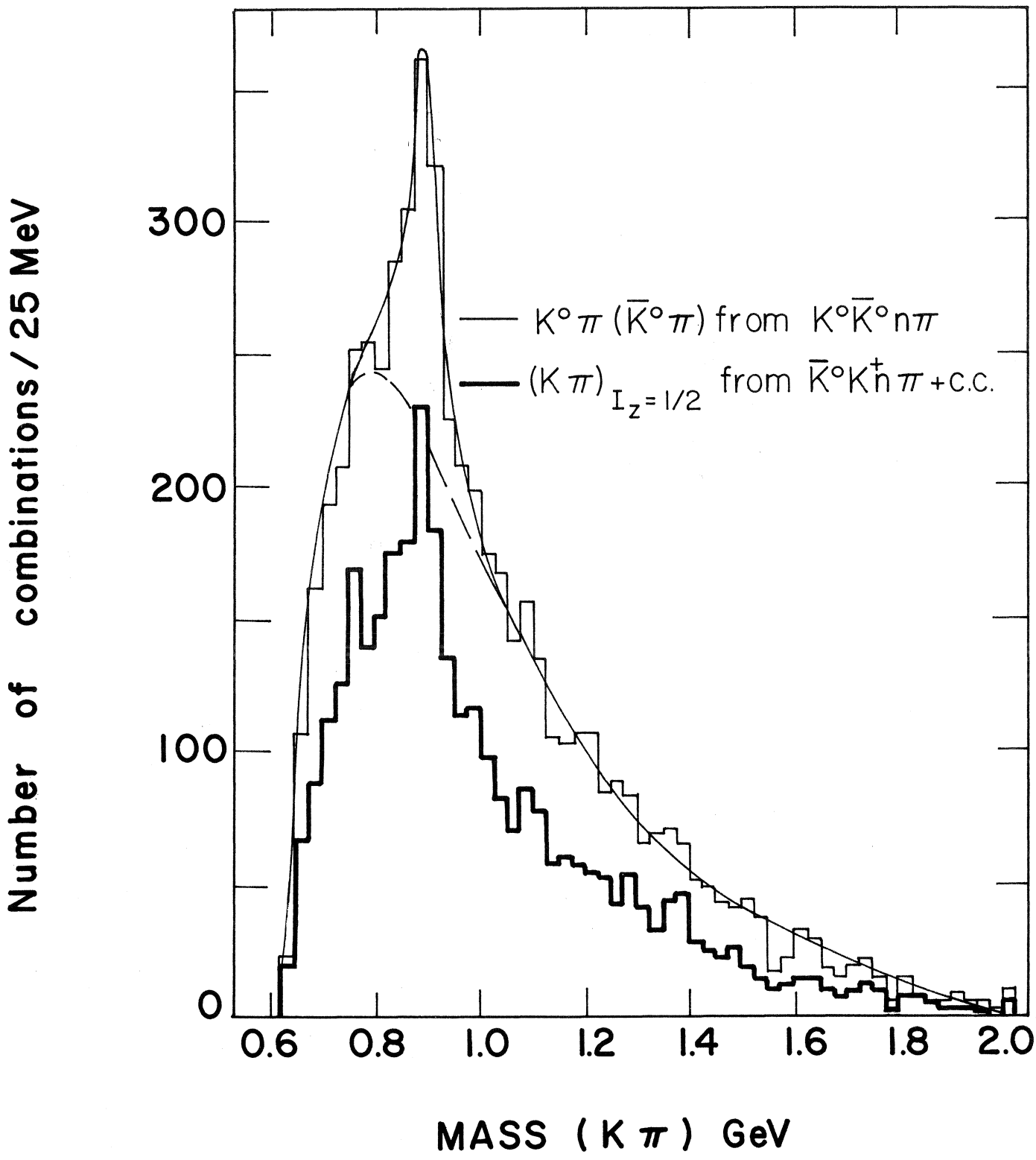
Number of combinations / 25 MeV
300
200
100
0
0.6
0.8
1.0
1.2
1.4
1.6
1.8
2.0
MASS (Kπ) GeV
K°π (K̄°π) from K°K̄°nπ
(Kπ) I_z = 1/2 from K̄°K⁺nπ + c.c.

fig. 1

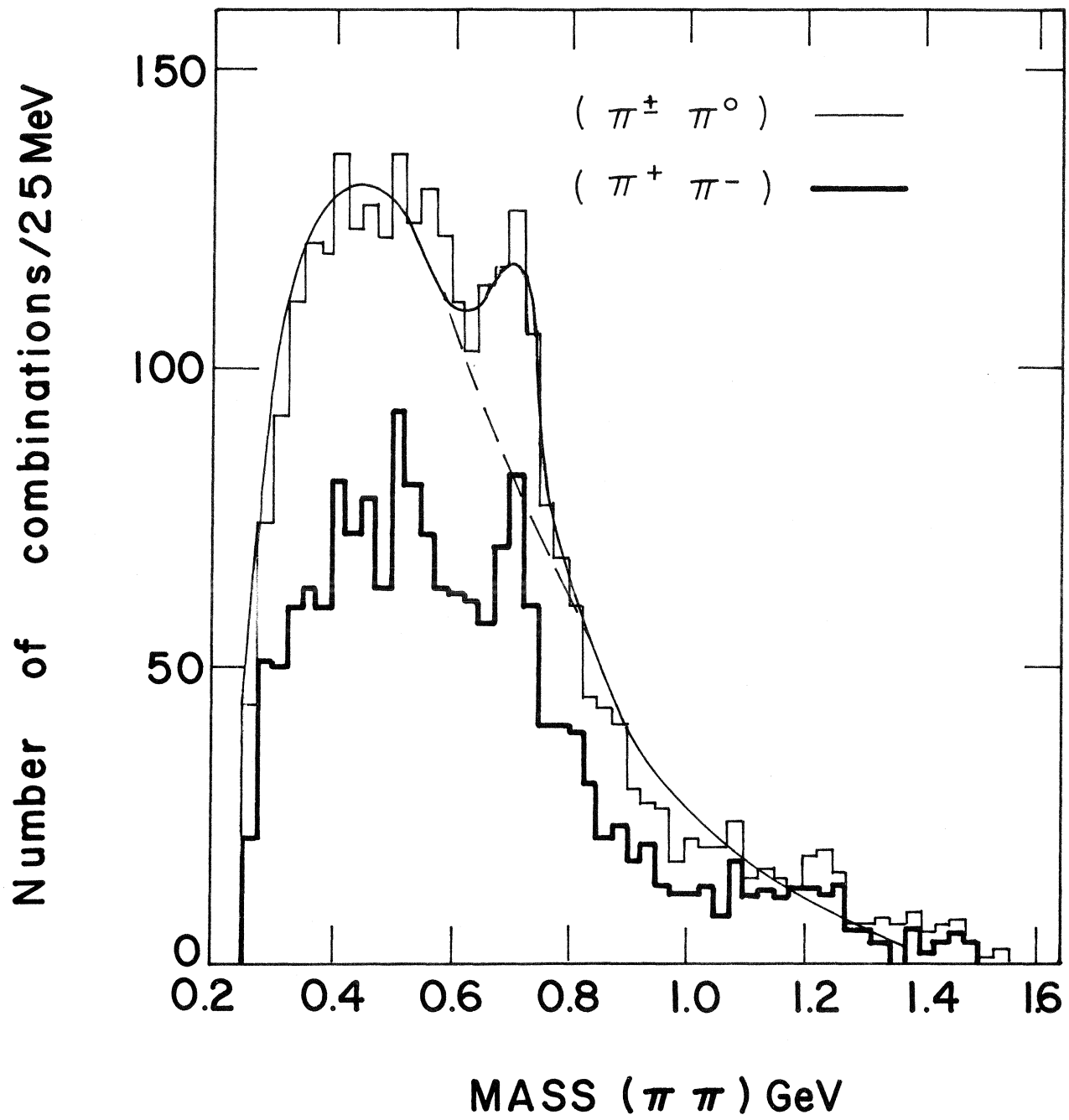
Number of combinations/25 MeV
150
100
50
0
0.2
0.4
0.6
0.8
1.0
1.2
1.4
1.6
MASS (π π) GeV
(π± π°)
(π+ π−)

fig. 2

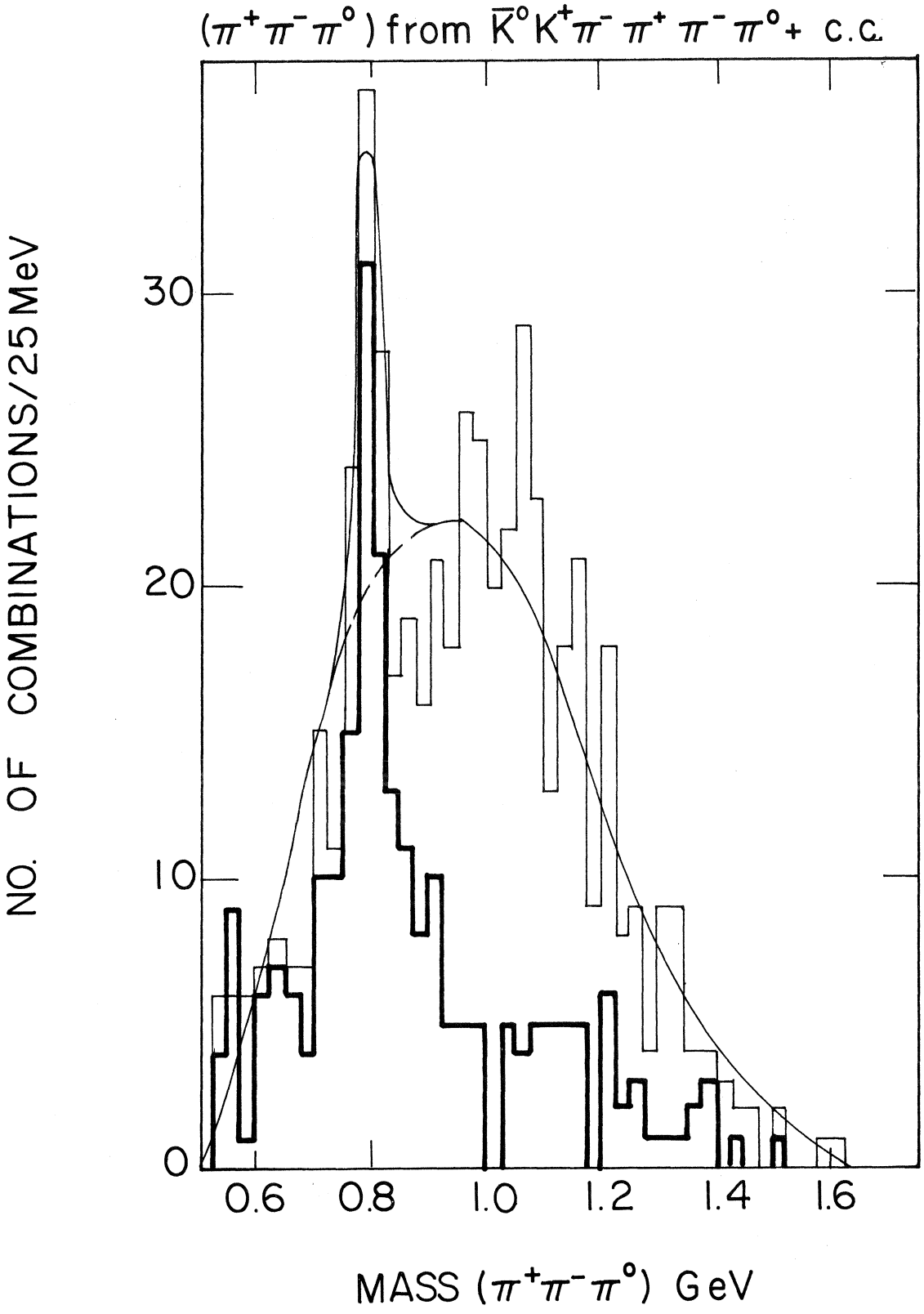
$(\pi^+\pi^-\pi^0)$ from $\bar{K}^0K^+\pi^-\pi^+\pi^-\pi^0$ + c.c.
NO. OF COMBINATIONS/25 MeV
0
10
20
30
0.6
0.8
1.0
1.2
1.4
1.6
MASS $(\pi^+\pi^-\pi^0)$ GeV

fig. 3

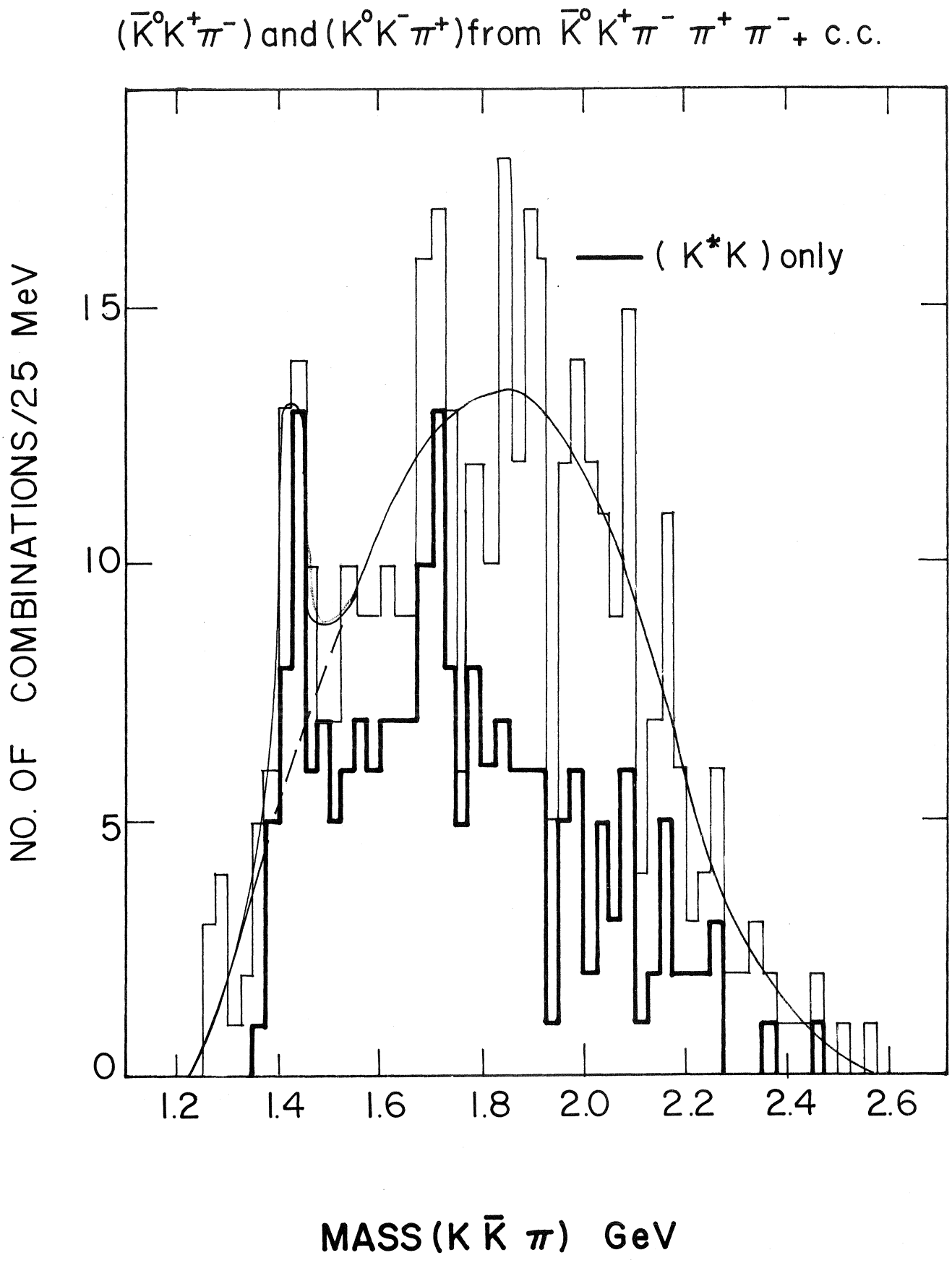
$(\bar{K}^0K^+\pi^-)$ and $(K^0K^-\pi^+)$ from $\bar{K}^0K^+\pi^-\pi^+\pi^-_+$ c.c.
(K*K) only
NO. OF COMBINATIONS/25 MeV
0
5
10
15
1.2
1.4
1.6
1.8
2.0
2.2
2.4
2.6
MASS (K $\bar{K}$ π) GeV

fig. 4

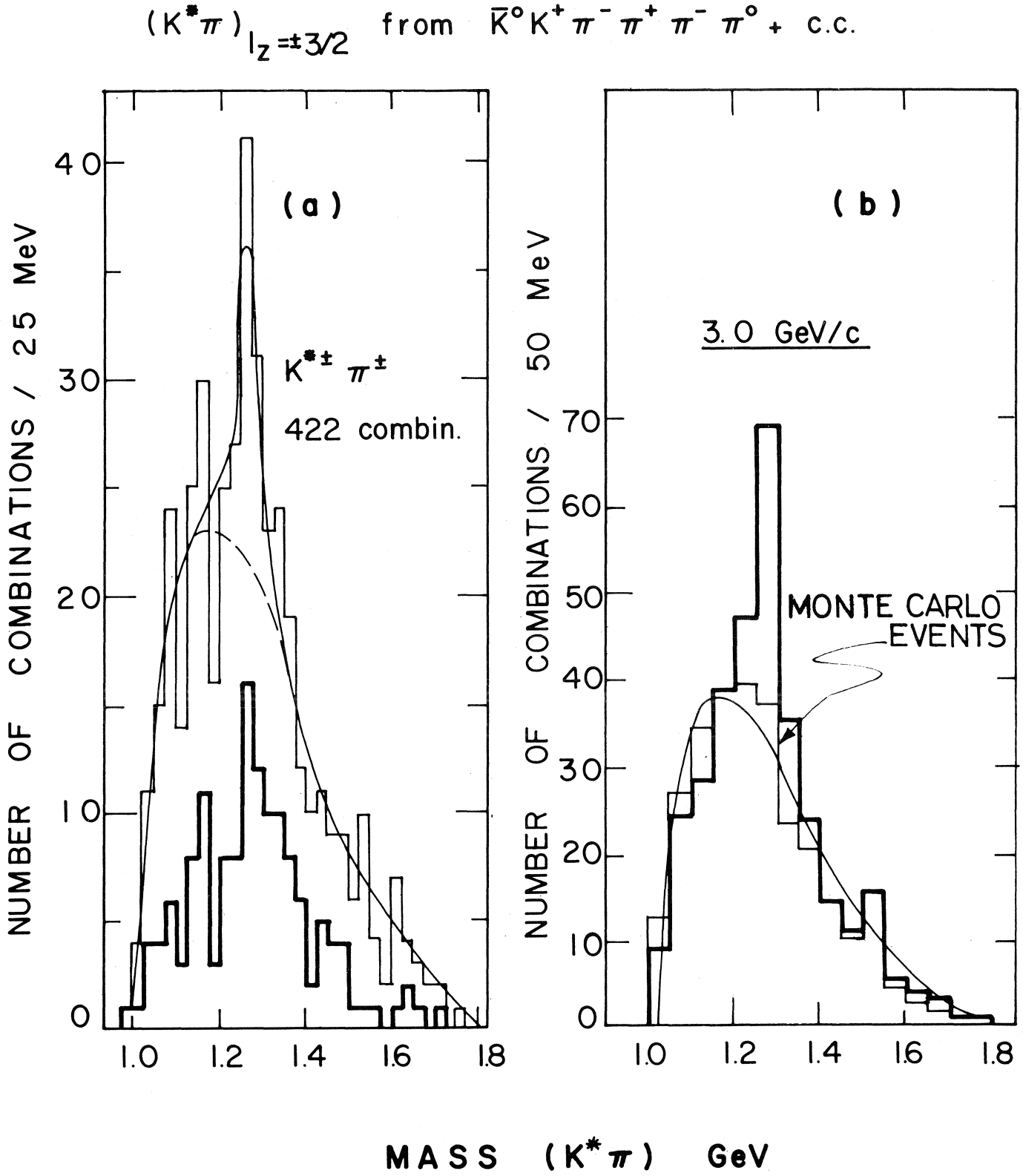
$(K^*\pi)_{I_z=\pm 3/2}$ from $\bar{K}^0 K^+ \pi^- \pi^+ \pi^- \pi^0$ + c.c.
(a)
$K^{*\pm}\pi^{\pm}$
422 combin.
(b)
3.0 GeV/c
MONTE CARLO EVENTS
NUMBER OF COMBINATIONS / 25 MeV
NUMBER OF COMBINATIONS / 50 MeV
MASS $(K^*\pi)$ GeV

fig. 5

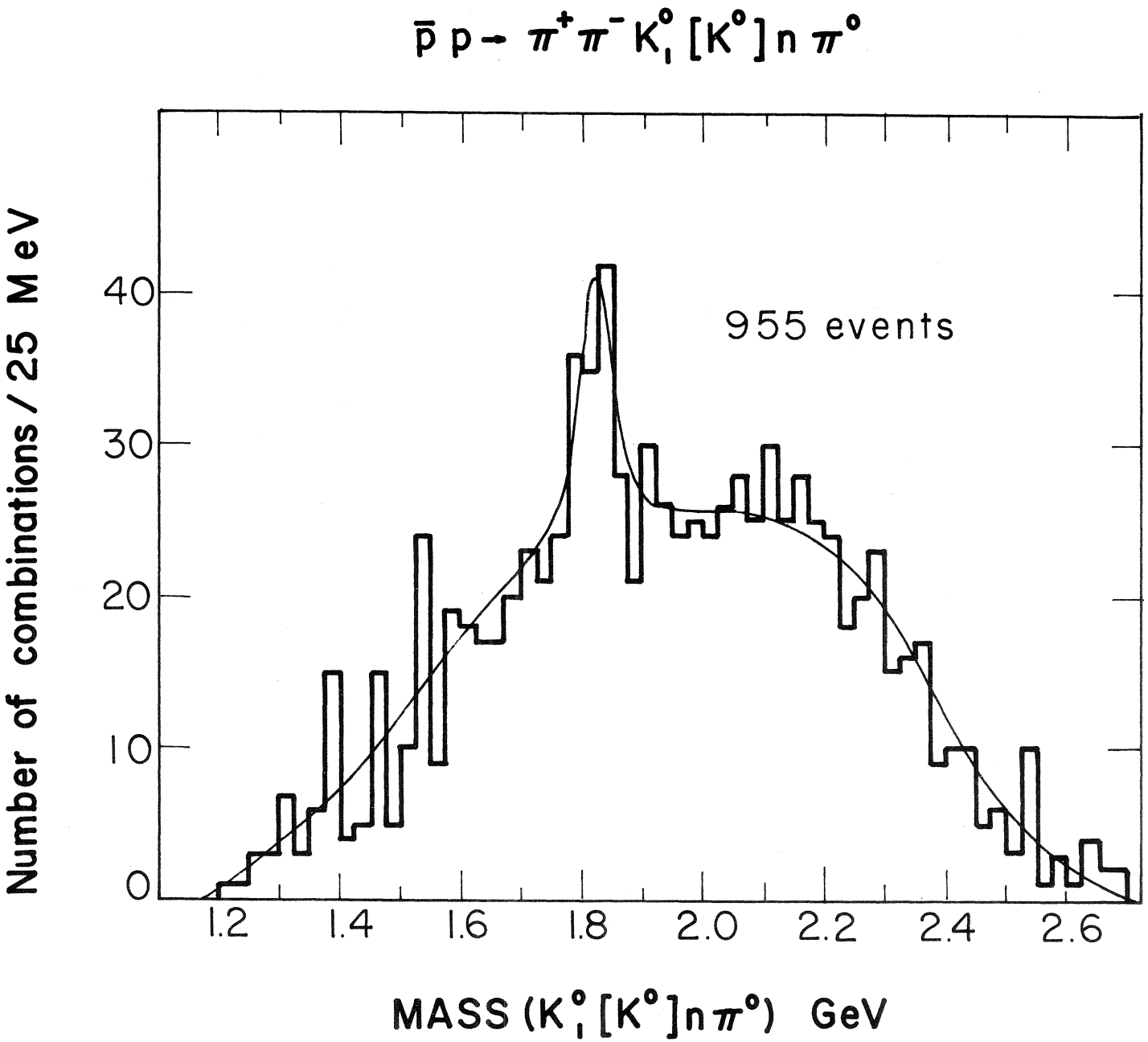
$\bar{p}\,p \to \pi^+\pi^- K^0_1[K^0]n\,\pi^0$
Number of combinations / 25 MeV
955 events
0
10
20
30
40
1.2
1.4
1.6
1.8
2.0
2.2
2.4
2.6
MASS ($K^0_1[K^0]n\,\pi^0$) GeV

fig. 6

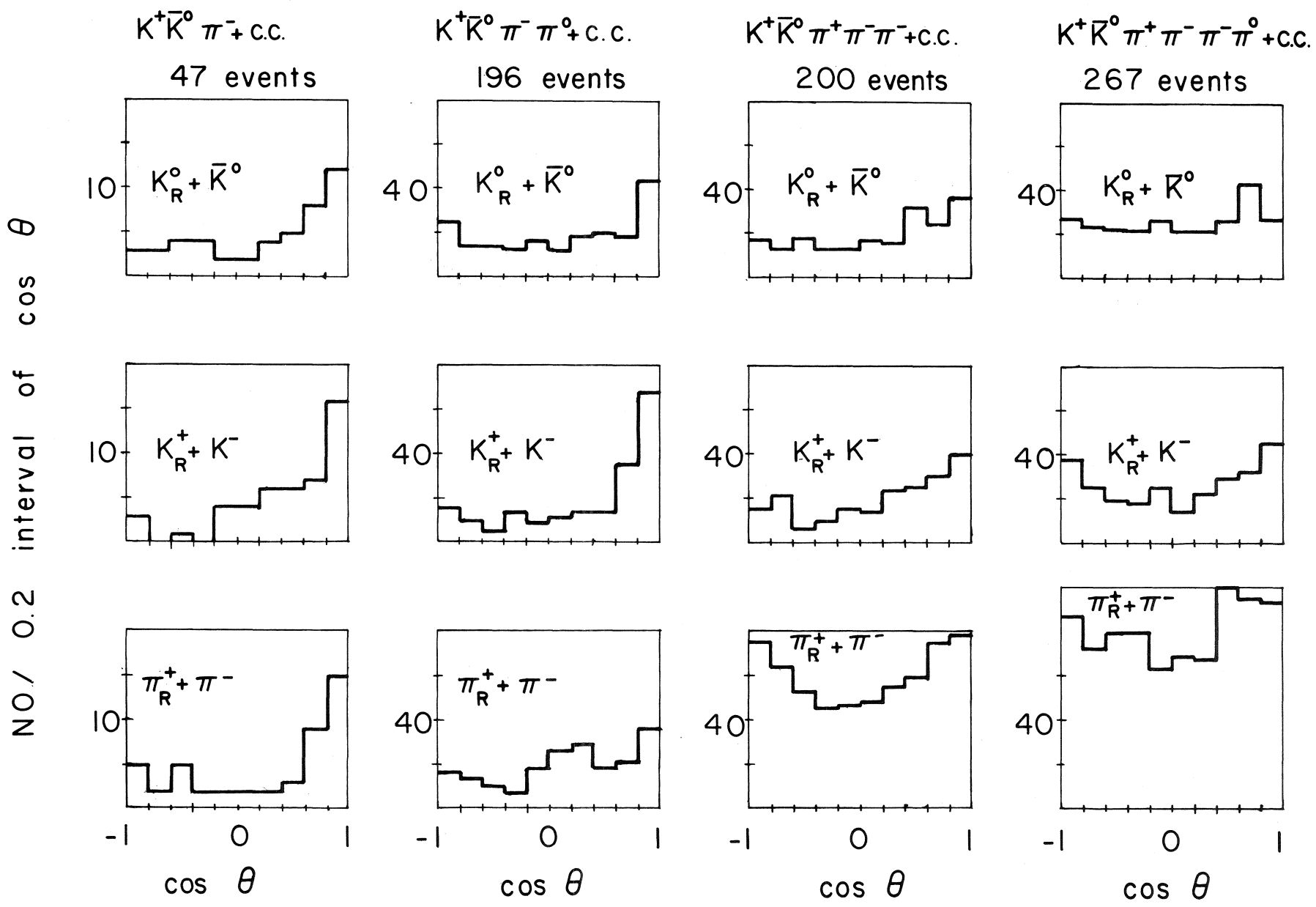
$K^+\bar{K}^0\pi^-$ + c.c.
47 events
$K^+\bar{K}^0\pi^-\pi^0$ + c.c.
196 events
$K^+\bar{K}^0\pi^+\pi^-\pi^-$ + c.c.
200 events
$K^+\bar{K}^0\pi^+\pi^-\pi^-\pi^0$ + c.c.
267 events
$K^0_R + \bar{K}^0$
$K^+_R + K^-$
$\pi^+_R + \pi^-$
NO / 0.2 interval of cos θ
10
40
-1
0
1
cos θ

fig. 7 a

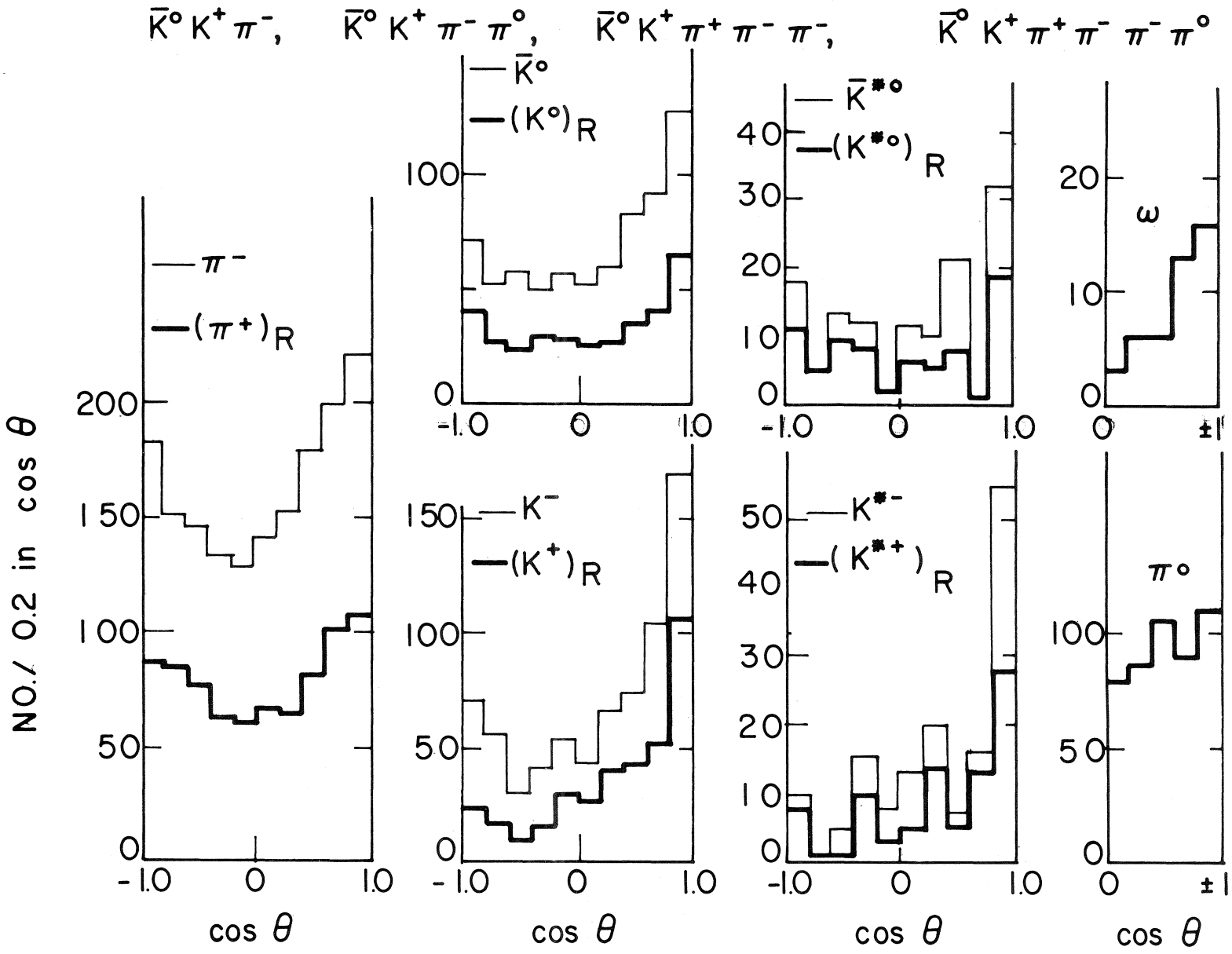
$\bar{K}^0 K^+ \pi^-$, $\bar{K}^0 K^+ \pi^- \pi^0$, $\bar{K}^0 K^+ \pi^+ \pi^- \pi^-$, $\bar{K}^0 K^+ \pi^+ \pi^- \pi^- \pi^0$
NO./ 0.2 in cos θ
π^-
$(\pi^+)_R$
$\bar{K}^0$
$(K^0)_R$
$\bar{K}^{*0}$
$(K^{*0})_R$
ω
K^-
$(K^+)_R$
K^{*-}
$(K^{*+})_R$
π°
cos θ

fig. 7 b

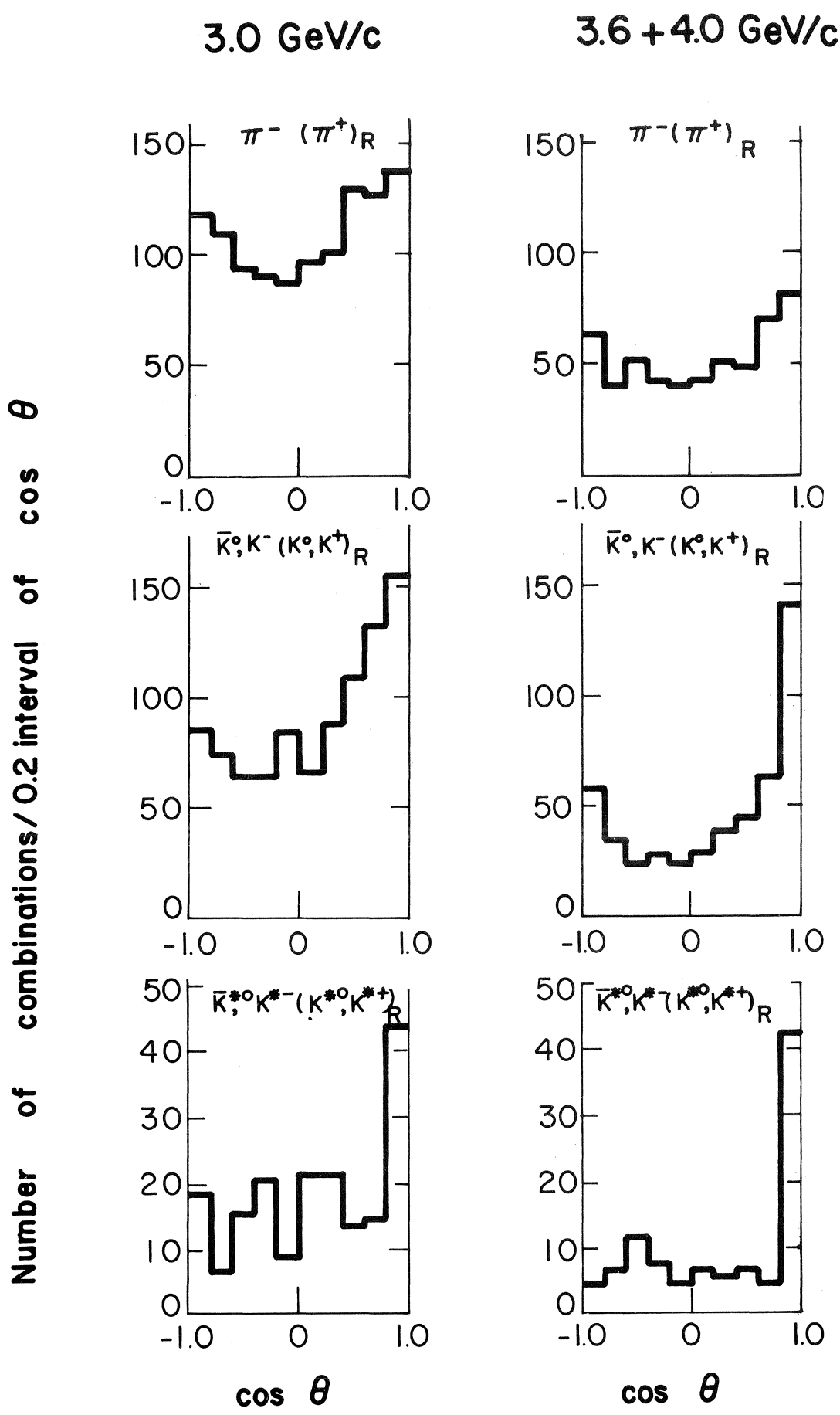
3.0 GeV/c
3.6 + 4.0 GeV/c
Number of combinations/0.2 interval of cos θ
π⁻ (π⁺)R
π⁻(π⁺)R
K̄°,K⁻ (K°,K⁺)R
K̄°,K⁻(K°,K⁺)R
K̄*°K*⁻(K*°K*⁺)R
K̄*°,K*⁻(K*°,K*⁺)R
150
100
50
0
40
30
20
10
-1.0
0
1.0
cos θ
cos θ

fig. 8

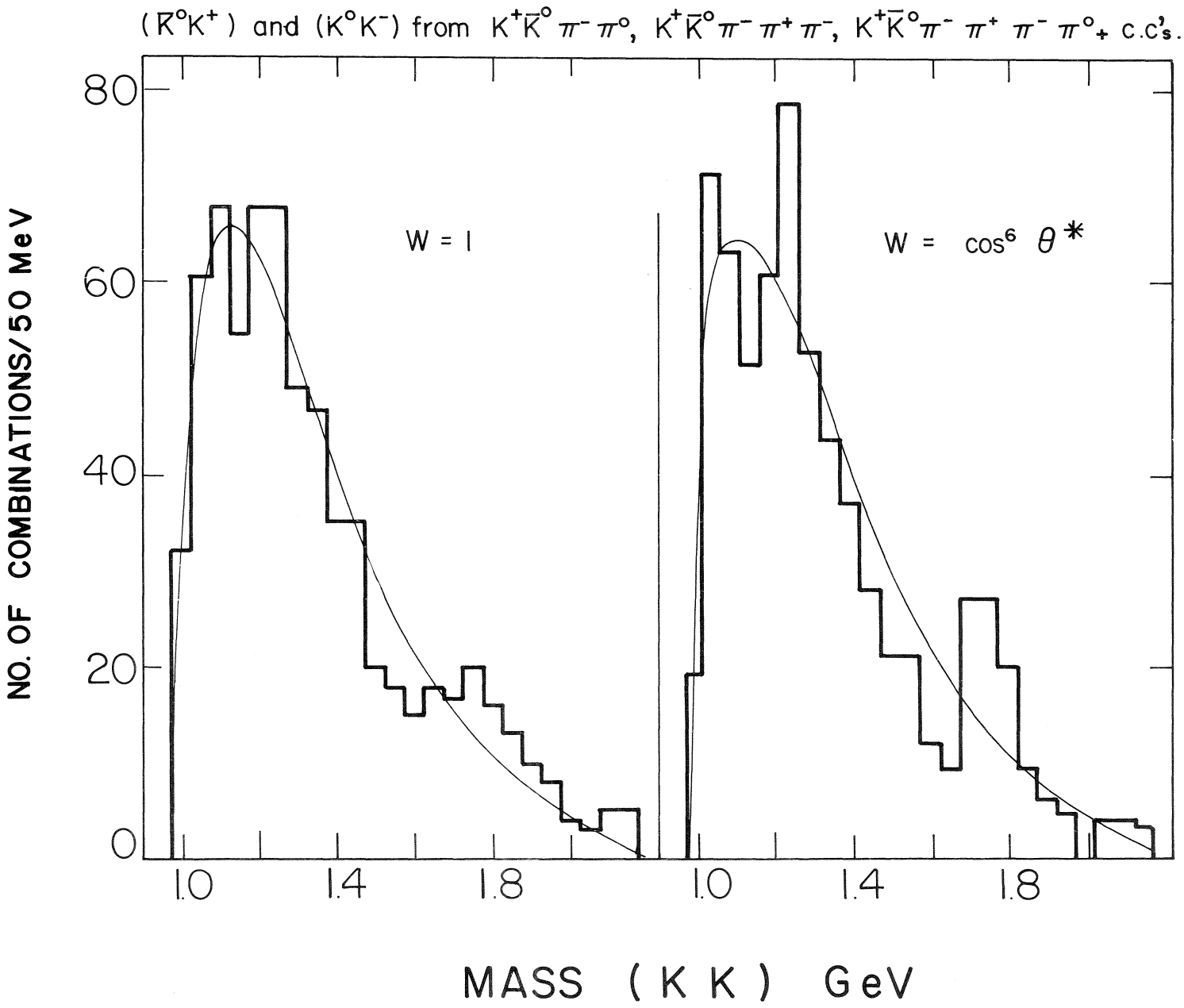
(K°K⁺) and (K°K⁻) from K⁺K°π⁻π°, K⁺K°π⁻π⁺π⁻, K⁺K°π⁻π⁺π⁻π°+ c.c's.
NO. OF COMBINATIONS/50 MeV
80
60
40
20
0
W = 1
W = cos⁶ θ*
1.0
1.4
1.8
1.0
1.4
1.8
MASS (K K) GeV

fig. 9

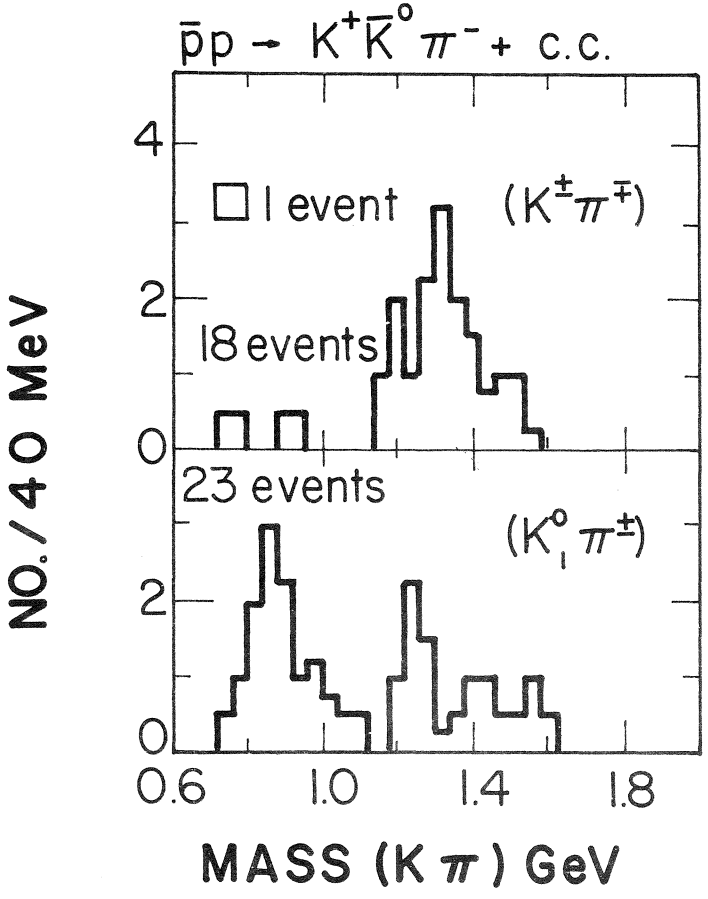
$\bar{p}p \to K^+\bar{K}^0\pi^- + c.c.$
1 event
$(K^\pm\pi^\mp)$
18 events
23 events
$(K^0_1\pi^\pm)$
NO./40 MeV
MASS $(K\pi)$ GeV

fig. 10

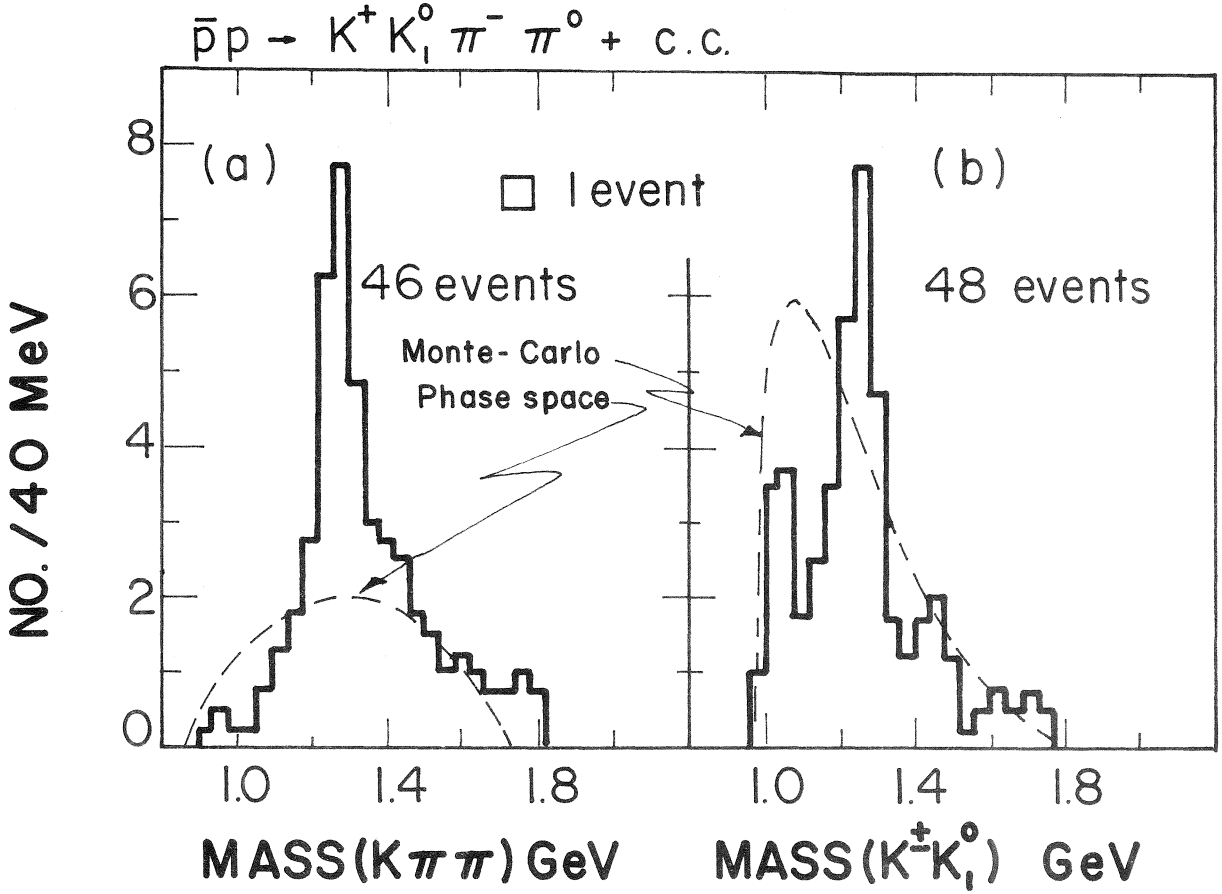
$\bar{p}p \to K^+K^0_1\pi^-\pi^0 + c.c.$
(a)
1 event
(b)
46 events
48 events
Monte-Carlo
Phase space
NO./40 MeV
MASS$(K\pi\pi)$ GeV
MASS$(K^\pm K^0_1)$ GeV

fig. 11

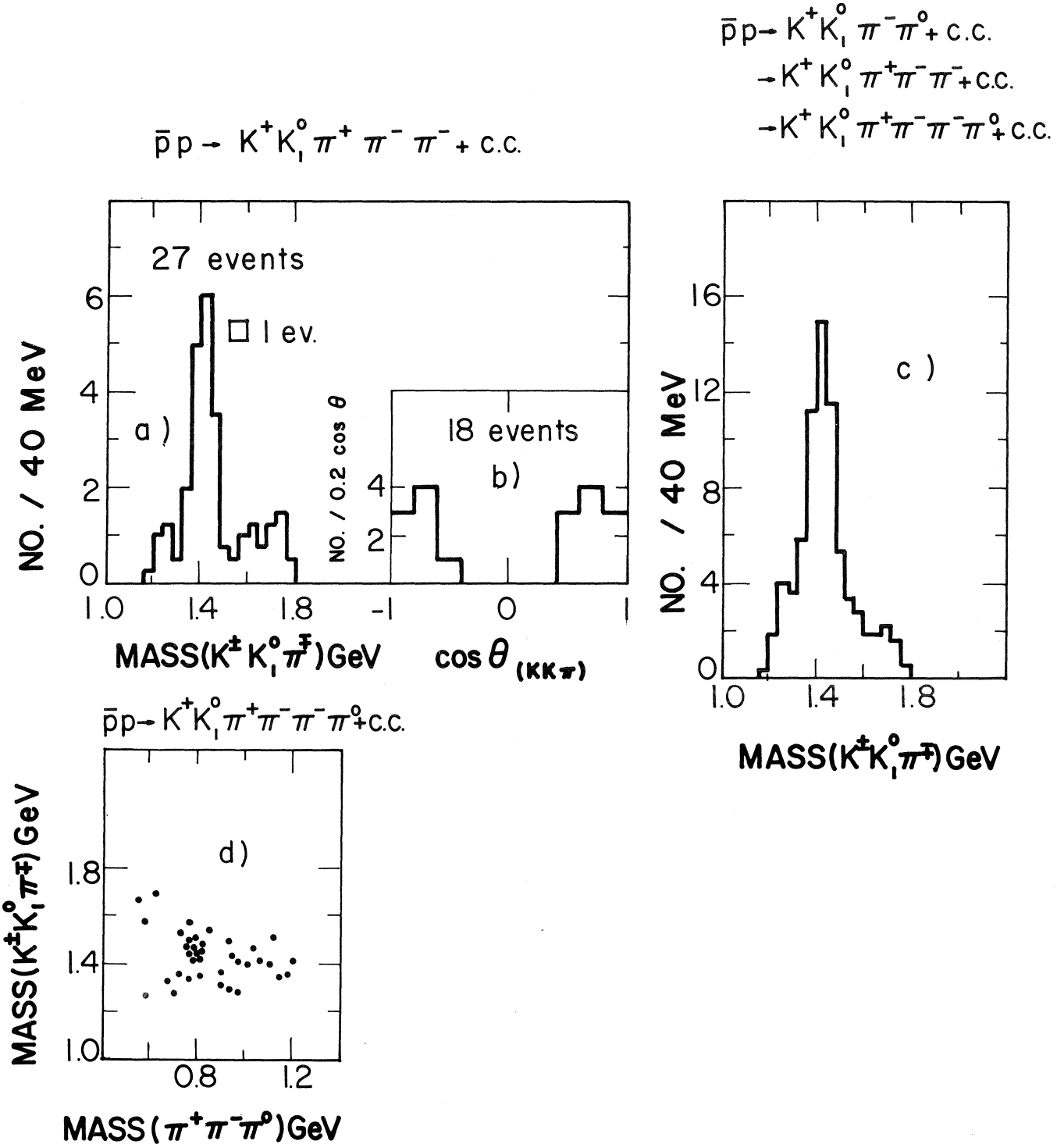
$\bar{p}p \to K^+K^0_1\pi^+\pi^-\pi^- + c.c.$
$\bar{p}p \to K^+K^0_1\pi^-\pi^0 + c.c.$
$\to K^+K^0_1\pi^+\pi^-\pi^- + c.c.$
$\to K^+K^0_1\pi^+\pi^-\pi^-\pi^0 + c.c.$
27 events
1 ev.
a)
18 events
b)
NO. / 40 MeV
NO. / 0.2 cos θ
MASS($K^\pm K^0_1\pi^\mp$) GeV
cos θ (KKπ)
c)
NO. / 40 MeV
MASS($K^\pm K^0_1\pi^\mp$) GeV
$\bar{p}p \to K^+K^0_1\pi^+\pi^-\pi^-\pi^0 + c.c.$
d)
MASS($K^\pm K^0_1\pi^\mp$) GeV
MASS($\pi^+\pi^-\pi^0$) GeV

fig. 12